ISIJ International, Vol. 46 (2006), No. 5, pp. 712–717

A New Physical Model for the Kinetics of the Bainite Transformation

Daniel GAUDE-FUGAROLAS and Pascal J. JACQUES

Université catholique de Louvain (UCL), IMAP, Place Sainte Barbe 2, B-1348 Louvain-la-Neuve, Belgium.

(*Received on August 29, 2005; accepted on February 23, 2006*)

A model describing the bainite reaction is presented that takes into account the effect of very small austenite grain size. This model considers the displacive approach and uses thermodynamic criteria for the description of the nucleation and growth of bainite sub-units forming either at grain boundaries or autocatalytically on previous sub-units. The evolution of the austenite composition with the partitioning and redistribution of carbon is estimated as the transformation proceeds. The size of the sub-units is calculated for each composition and temperature.

The transformation kinetics, as well as the incomplete reaction phenomenon, are correctly predicted. Furthermore, the influence of the austenite grain size on the bainite transformation rate is addressed in the case of austenite grains smaller than the length of an unconstrained bainite sub-unit. In this case, the observed enhanced nucleation rate is semi-empirically related to the austenite yield strength. This semi-empirical relationship is corroborated with kinetics data from different alloys.

KEY WORDS: bainite; kinetics; model; autocatalysis; carbon redistribution; grain size.

1. Introduction

Due to an increasing demand for advanced bainitic steels, it is necessary to achieve a better understanding of the formation mechanism of this phase. Once considered as a deleterious phase in quenched structural components, bainite becomes more and more one of, or even the, target phase in the microstructure of high-performance alloys like cast irons, weld steels and also high-strength low-alloy TRIP-assisted multiphase steels.

Different mechanisms have been proposed for the bainite formation[1–4] but only a few quantitative models can predict the reaction kinetics.[5–8] When considered to be a displacive transformation, the bainite reaction involves the repeated nucleation and growth of small sub-units of supersaturated bainitic ferrite, followed by the redistribution of carbon into the surrounding untransformed austenite.[9] Due to this carbon redistribution the bainite transformation may stop before the complete austenite transformation. Indeed, the incomplete reaction phenomenon occurs when the austenite carbon content reaches the T_0 curve, *i.e.* the locus where austenite and ferrite of the same composition have the same Gibbs free energy.[9]

The effect of the austenite composition and grain size, the carbon redistribution, the entrapment of carbon-enriched austenite films between bainite sub-units[10–12] and the role of newly formed bainite sub-units as potential nucleation sites (autocatalysis or sympathetic nucleation)[5,13–15] are all issues that need to be considered in a model describing this reaction. Furthermore, the extreme case of very small austenite grains that constrain the growth of the bainite sub-units is particularly interesting, since it may involve the interaction of the strains generated during the transformation with the transformation kinetics, and an early soft impingement. Hitherto, the bainite transformation in small grains has been hardly referred in the literature.

The purpose of the present study is to assess a model that addresses the above-mentioned issues and is able to predict the transformation kinetics of the bainite reaction and the final volume fractions of bainite, retained austenite and carbon-enriched austenite films for a wide range of steels.

2. Description of the Model

2.1. Overview

As already advanced in the introduction, the bainitic transformation is a complex process, and even a simplified description needs to consider a large number of events. The reaction starts with the nucleation of a sub-unit at the boundary of the austenite grain, which lengthens until its growth is restrained by plastic deformation of the austenite matrix. Other sub-units nucleate at the tip of this sub-unit, and as this process keeps repeating itself to end up forming the characteristic sheaf structure of bainite. As for Widmanstatten ferrite, carbon partitions during nucleation, but the development of a nuclei into a bainite sub-unit is a diffusionless process. It is only after the growth of a bainite sub-unit has stopped that carbon partitions and redistributes in the remaining austenite matrix. Due to the intervals between nucleation events the overall growth rate of the sheaf is very different to that of the individual sub-units. Several sheafs may form simultaneously in different regions of the grain, contributing to the total amount of bainite created.[9]

The bainite reaction is therefore a nucleation-controlled

transformation. The growth of individual sub-units is so fast that for the purpose of this model it can be assumed to be instantaneous. Hence, the method used in this work to calculate the kinetics of the bainite transformation consists in determining in the first place the maximum number of nucleation events potentially occurring in each time interval, and then use thermodynamic criteria to find how many of them successfully develop into bainite sub-units.

2.2. Thermodynamics of Nucleation

During the decomposition of austenite into an equilibrium mixture of ferrite and carbon enriched austenite there is a substantial change in chemical composition. However, the formation of a ferrite nucleus in an austenitic matrix involves such a very small volume of material that it cannot possibly be considered to affect the composition of the remaining austenite. Keeping that in mind it is possible to determine the maximum possible free energy change for nucleation ΔG_m (Fig. 6.2, pp. 130 of Ref. 9)). It is observed however, that to observe nucleation leading to a displacive transformation ΔG_m needs to be larger (in absolute values) than the "universal nucleation function", G_N, as defined by Ali and Bhadeshia[9,16]:

$$G_N = 3.637(T - 273.18) - 2\,540 \quad \text{.....(1)}$$

where T is the absolute temperature.

The criterium for the nucleation of a bainite nucleus has been integrated in the model using the function

$$\mathcal{F}_n = \begin{cases} \tanh\left(-\dfrac{\Delta G_m - G_N}{RT}\right): & (\Delta G_m - G_N) < 0 \\ 0: & (\Delta G_m - G_N) \geq 0 \end{cases} \quad \text{....(2)}$$

which provides a simple way to describe smoothly the complete transition from no nucleation till site saturation.

2.3. Primary Nucleation

It is defined as primary the nucleation that occurs at the austenite grain boundaries. Analogously to the case of martensite nucleation, bainite primary nucleation occurs on surface defects present on austenite grain boundaries. The parameter N_0 is defined as a surface density of potential nucleation sites. As this parameter would be difficult to measure it is used as one of the adjustable parameters of the model. As the reaction proceeds, the austenite grain boundary area decreases as austenite is consumed by the transformation. The remaining austenite grain boundary area, s_γ, can be estimated from the total grain boundary area, S_γ, and the volume fraction of remaining austenite, v_γ, as $s_\gamma = S_\gamma \cdot v_\gamma^{2/3}$.

The number of successful (primary) nucleation events occurring during a time interval $d\tau$ is therefore estimated as

$$dI_p = N_0 \cdot s_\gamma \cdot \nu \cdot \mathcal{F}_n \cdot d\tau \quad \text{.....(3)}$$

where ν is an attempt frequency reflecting the thermal agitation of the atoms. The attempt frequency is $\nu = k \cdot T/\hbar$ with k the Boltzmann constant, $\hbar$ the Planck constant and T the absolute temperature.

2.4. Autocatalytic Nucleation

Autocatalytic nucleation occurs at the tip of already formed bainite sub-units. As new sub-units repeatedly form at the end of existing ones, the usual sheaf structure of bainite develops. This process always starts with a primarily nucleated sub-unit, and eventually finishes by the last sub-unit impinging on the grain boundary. As the average length of a sheaf that develops in a grain of diameter D_γ is $2D_\gamma/\pi$, the number of sub-units in such sheaf will be roughly proportional to $2D_\gamma/(\pi \cdot l_b)$, where l_b is the length of a single sub-unit. The proportionality factor β_a is one of the adjustable parameters of the model, and accounts for the misorientation between bainite sub-units and the sheaf and for the possibility that more than one sub-unit is nucleated in each autocatalytic nucleation event. The amount of successful (autocatalytic) nucleation events occurring in a time interval $d\tau$ is therefore estimated as

$$dI_a = I_p \cdot \frac{2 \cdot D_\gamma}{\pi \cdot l_b} \cdot \beta_a \cdot \mathcal{F}_n \cdot d\tau \quad \text{.....(4)}$$

2.5. Bainite Sub-unit

Bainite sub-units are considered to have a lenticular shape. The size of each bainite sub-unit is defined in the model by its thickness and aspect ratio. The thickness of a bainite sub-unit has been described as a function of temperature, driving force for transformation and yield strength of austenite by Singh and Bhadeshia.[17] The average aspect ratio of bainite sub-units has been characterised by Wang *et al.* for a large range of alloys.[18] In the case that bainite growth is constrained by austenite grain size the model will adjust the size of the sub-unit because bainite cannot grow across grain boundaries.

2.6. Bainite Fraction Formed

Once the bainite nucleus has formed, there needs to be enough driving force to sustain partitionless transformation from austenite to ferrite for the nucleus to develop into a sub-unit. $\Delta G_{np}^{\gamma \to \alpha}$ is the free energy change for diffusionless transformation from austenite to ferrite, parameter that controls the probability of a nuclei to develop into a sub-unit, as described (Fig. 6.2, pp. 130 of Ref. 9)). The amount of bainite formed during a time interval $d\tau$ is therefore given by

$$dv_b^e = (I_p + I_a) \cdot u_b \cdot \exp\left(-\frac{G_{np}^{\gamma \to \alpha}}{RT}\right) \cdot d\tau \quad \text{.....(5)}$$

where I_p and I_a are, respectively, the primary and autocatalytic contributions of successful nucleation events. u_b is the volume of one bainite sub-unit. R and T are the gas constant and absolute temperature.

A method based on Avrami's extended volume correction[19] has been used to account for nucleation site depletion and impingement of developing sub-units. The total volume of new bainite sub-units created during each time interval is corrected by the volume fraction of remaining austenite as,

$$dv_b^r = v_\gamma dv_b^e \quad \text{.....(6)}$$

where dv_b^e is the extended volume of bainite created during an interval $d\tau$, v_γ is the volume fraction of remaining austenite and dv_b^r the real volume of bainite formed during

that interval.

2.7. Carbon Redistribution

As described earlier, the development of a bainite sub-unit occurs diffusionlessly, and it is only after its growth has stopped that carbon partitions. The partitioning of carbon can either produce a distribution of carbides or, in high silicon alloys, can redistribute into the remaining austenite without precipitation.[9] This model only deals with the second case, in which all the partitioning carbon is redistributed in the remaining austenite.

The degree of homogeneity of the carbon redistribution depends on the mobility of carbon and on microstructural aspects. As the bainite reaction happens at temperatures for which the mobility of carbon is low, the redistribution of carbon in austenite tends to be inhomogeneous. It has often been observed that films of carbon-enriched austenite become trapped between bainite sub-units.[6,9,10] The composition of these austenite films is close to the value given by the Ae'_3 curve[6] (*i.e.* the composition of the $(\alpha+\gamma)/\gamma$ phase boundary in paraequilibrium conditions). The carbon-enriched austenite films act as reservoirs of carbon, preventing it to enrich the remaining austenite. The end of the bainite reaction is thus postponed.

The volume fraction of austenite trapped as thin films between sub-units depends on the volume fraction of bainite formed.[10] Although the thickness of these films varies slightly with temperature,[10,11] the model presented here considers, as a first approximation, that the volume fraction of enriched austenite v_h is proportional to the bainite volume fraction. The proportionality parameter, which is one of the fitting parameters of the model, is adjusted so that the volume fraction of enriched austenite is limited to an upper boundary of 12% of the volume fraction of bainite, keeping it consistent with published literature.[5,6,10]

2.8. Transformation in Small Austenite Grains

The model presented so far describes accurately the transformation of austenite into bainite when the austenite grains are large with respect to the size of the bainite sub-units. However, in the case of austenite grain size of the same order than the length of a bainite sub-units, the final size of these sub-units will be constrained by the size of the austenite grains.

During the transformation in these 'small' grains, several changes will be induced in the morphology and kinetics of the reaction. Most of them are already taken into account in the model. First, the larger proportion of austenite grain boundary area will promote primary nucleation. However, impingement with the boundaries of the austenite grains will inhibit autocatalytic nucleation,[20] and the length of the bainite sub-units will be eventually limited by the size of the austenite grains.[21] Finally, as impingement forces bainite sub-units to grow parallel to each other (as described by Jacques,[20] minimisation of the transformation strains by the growth of an optimal combination of different bainite variants is no longer possible, as it would happen in larger grains,[9,22] and some transformation stresses may build up as the reaction proceeds.

Only the effect of internal stress needs to be considered, as the rest are already included in the formulation of the model. It is well known that external and internal stresses affect the kinetics of many transformations, and particularly of the bainite reaction, by an enhancement of the nucleation rate.[23–28] The effect of the stresses generated during the transformation can therefore be described by including an additional term in the definition of the density of potential nucleation sites per unit surface N_0. This term takes the form of an enhanced activation rate, in which the activation energy is a function of the austenite yield strength, σ_y.[29]

$$N_0 = N_s \exp\left(-\frac{B_s \cdot \sigma_y}{R \cdot T}\right) \quad \text{.....(7)}$$

where σ_y is the austenite yield strength; B_s is a function that describes the tensile state of the parent austenite; N_s is a potential nucleation site surface density and R and T have their usual meanings. As more work is still needed to characterise B_s and N_s thoroughly, they are only used presently as fitting parameters of the model.

3. Validation of the Model and Discussion

3.1. Fitting Parameters

The present model uses the following fitting parameters:

(i) The surface density of potential nucleation sites N_0. It has been fitted to $N_0 = 2.0 \cdot 10^{-4}$ nuclei m^{-2}. It would be expected that N_0 is related to the surface energy of the boundary, and therefore changes with composition and stress state.

(ii) The proportionality factor β_a accounts for the misorientation between bainite sub-units and the sheaf and for the possibility that more than one sub-unit is nucleated in each autocatalytic nucleation event. This value has been treated as an adjustable parameter and its value fitted to $\beta_a = 1.5$ as a realistic value.

(iii) The thickness of each one of the carbon-enriched austenite films trapped between bainite sheaves is a parameter difficult to evaluate. In the present model, it has been restricted to an upper boundary of 6% of the thickness of a bainite sub-unit. Even though this value is above the values found in literature it is still in the same order of magnitude.[5,6,10]

(iv) Finally, the nucleation rate in the case of small austenite grains still needs to be better understood. In the present model, it is described using a semi-empirical function defined with two adjustable parameters: B_s, which is believed to describe the stress state of the parent austenite and N_s, which is the pre-exponential parameter of the enhanced surface density of potential nucleation sites. As for the parameter (i), these parameters need to be characterised for each alloy composition, but they are only needed in the case of small austenite grains. The values adjusted for the studied alloys are shown in **Table 2**.

3.2. Validation

3.2.1. Experimental Data

In order to assess the validity of the model, its predictions are compared with published experimental data of the bainite transformation kinetics. The chemical composition of the investigated alloys is given in **Table 1**. All steels except steel D steels contain some silicon to inhibit cementite

precipitation from austenite during the bainite transformation.[9] Steel A has been used to validate and adjust the fitting parameters of the general model (items (i) to (iii) in Sec. 3.1), and steels B, C and D have been used to study the special case of transformation occurring in small austenite grains. Steel A was either austenitised for 15 minutes to obtain an austenite grain size of about 50 μm, or thermally cycled to obtain an austenite grain size of 8 μm. Steels B, C and D were intercritically annealed to generate a microstructure containing ferrite and small austenite grains with an average size of 2 μm and various carbon contents. The specimens were then rapidly quenched to the bainite transformation temperature and isothermally transformed. Specimens of the studied alloys were held at different temperatures between 310 and 460°C. The heat treatments were conducted in a dilatometer that continuously measured the change in length of the specimens. The microstructure of the different specimens was characterised by TEM or SEM and the volume fraction of retained austenite and its carbon content was measured by X-ray diffraction and Mössbauer spectroscopy.[20,30,31]

Table 1. Chemical composition and austenite grain size of the investigated steels.

/wt.%	C	C in γ	Mn	Si	Al	γ grain size /μm
Steel A	0.58	0.58	1.66	1.35	0.03	8, 50
Steel B	0.29	0.58	1.42	1.41	0.04	2
Steel C	0.11	0.29	1.50	1.53	0.04	2
Steel D	0.16	0.64	1.30	0.38	0.03	2

The carbon content of the austenite phase is specified due to the dual microstructure (intercritical austenite+ferrite) of some of the alloys studied.

Table 2. Parameters describing the surface density of potential nuclei for the investigated steels.

	N_s	B_s	γ grain size /μm	l_b/D_γ
Steel A	$2.0 \cdot 10^{-4}$	0	50	0.04
Steel A	$2.0 \cdot 10^{-4}$	0	8	0.4
Steel B	$1.07 \cdot 10^{4}$	274.5	2	1.8
Steel C	$2.11 \cdot 10^{4}$	324.6	2	1.7
Steel D	$9.74 \cdot 10^{4}$	301.3	2	1.8

N_s has the units of surface density of potential nuclei, that is nuclei$\cdot$m^{-2}. l_b/D_γ is the calculated length of a bainite sub-unit at the beginning of the transformation (in the case of small austenite grains, unconstrained by the size of the austenite grain) divided by the diameter of the austenite grain.

3.2.2. Overall Transformation Kinetics

Figure 1 compares the predicted evolution of the bainite reaction with the experimental data for steel A with an austenite grain size of 8 μm held at 360°C. The model predicts correctly that the reaction first accelerates with the increasing volume fraction of bainite, and then decreases asymptotically up to the final bainite volume fraction described by the T_0' curve (incomplete reaction). It is worth reminding that the volume fraction of bainite when the transformation stops is not one of the inputs of the model, but is correctly predicted by the thermodynamic criteria and by the calculated increasing carbon content of the remaining austenite.

3.2.3. Effect of Temperature and Grain size

Figures 2(a) to 2(c) present the experimental and predicted times for achieving bainite transformation levels of 30% and 60% and the maximum bainite volume fraction obtained when the incomplete reaction phenomenon occurs in steels A and B. The considered austenite grain sizes are 2, 8 and 50 μm, and the temperatures of the isothermal heat treatments are 310, 360, 410 and 460°C, respectively.

The time for the several degrees of transformation is remarkably well predicted for the different grain sizes. The prediction of the final volume fraction of bainite (incomplete reaction phenomenon), presents a varying degree of accuracy. The assumption that carbon partitions rapidly into

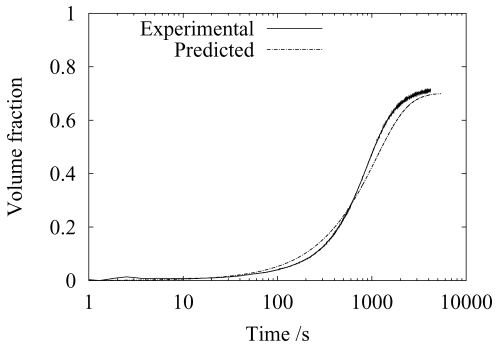

Fig. 1. Experimental and predicted kinetics of isothermal bainite transformation at 360±C for steel A with an austenite grain size of 8 μm.

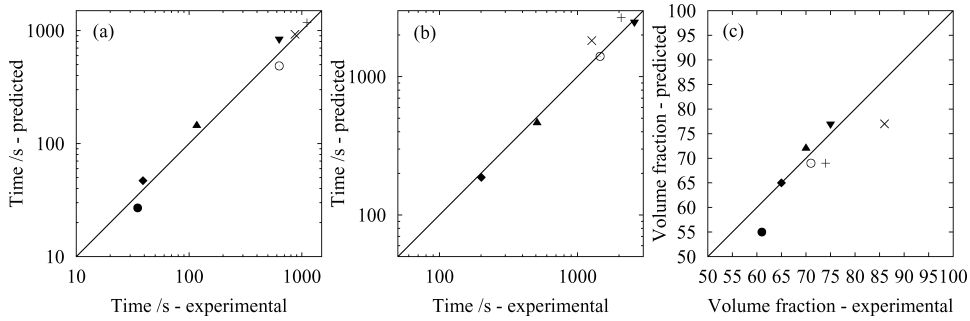

Fig. 2. Predictions *vs.* experimental values of the time needed to reach (a) 30% of transformation, (b) 60% of transformation and (c) of maximum volume fraction of bainite. ▼ grain size 2 μm at 310°C; ▲ grain size 2 μm at 360°C; ◆ grain size 2 μm at 410°C; ● grain size 2 μm at 460°C; ○ grain size 8 μm at 360°C; ×grain size 50 μm at 310°C; +grain size 50 μm at 360°C.

the remaining austenite, and redistributes evenly is a simplification that can explain these discrepancies. As shown by the differences in accuracy, this assumption is better suited for small grains for which diffusion distances are shorter and for higher temperatures when mobility of carbon is enhanced. It may also be postulated that this discrepancy results from the carbide precipitation within the bainitic ferrite observed in the case of the larger austenite grains.[20)]

3.2.4. Effect of Composition on Nucleation in Small Grains

As stated earlier, it was expected that in all cases where austenite grain is smaller than the unconstrained bainite sub-unit, nucleation will be better described by a function N_0 of the type shown in Eq. (7), and that has already been validated using kinetics data of steels A and B. However, is was also expected that as primary nucleation rate is related to the surface energy of the austenite grain boundary, the parameters of such equation would depend on the composition of the alloy. As a preliminary study of this effect, kinetic data of steels C and D have been considered. Steel C has virtually the same manganese and silicon content in austenite as steels A and B but a different carbon content in austenite.[31)] Steel D has a similar carbon and manganese content, but a reduced silicon content. Furthermore, the silicon content of steel D is not high enough to avoid carbide precipitation from austenite, so that the incomplete reaction phenomenon is not observed.[30)] For this alloy, the model was modified to account for the lack of carbon enrichment of the austenite matrix. In both cases, the resulting values of the surface density of potential nucleation sites, N_0, fit comfortably to an expression of the type of Eq. (7), as shown in **Fig. 3**. The parameters of such equation for each alloy are also shown in Table. The underlaying phenomena are nevertheless complex, and more work is needed to characterise the nucleation behaviour of bainite in small austenite grains.

3.2.5. Carbon Redistribution

The carbon content of retained austenite in steel B, experimentally determined after the bainite reaction has stopped, has been plotted in **Fig. 4** with the T_0 curve and with the austenite carbon content as predicted by the model. The T_0 curve has been determined using algorithms developed by Bhadeshia and coworkers.[9,32)] This plot shows that although the nucleation and growth of bainite should stop when the composition of the parent austenite reaches the composition of the T_0 curve, post-transformation austenite presents a composition slightly beyond that value. The carbon expelled from the bainite sub-units that form right before the parent austenite reaches the T_0 composition pushes the final composition of austenite beyond that critical value.

The model describes correctly not only the carbon enrichment of austenite, but also this enrichment beyond the T_0 curve. The accuracy of the prediction in reactions occurring at medium and high temperatures is remarkable, although as the reaction temperature is lowered the model tends to overestimate the carbon enrichment of the untransformed austenite.

This is again a consequence of the assumption that carbon redistributes rapidly and evenly at all temperatures, without taking into account the reduced mobility of carbon at lower temperatures, when the the fact is that the diffusion coefficient of carbon in austenite varies by about two orders of magnitude between 300°C, and 450°C.

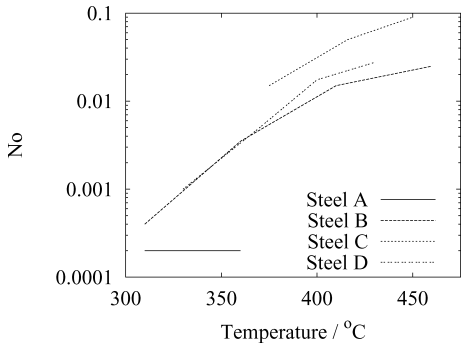

Fig. 3. Nucleation parameter N_0 for different steels.

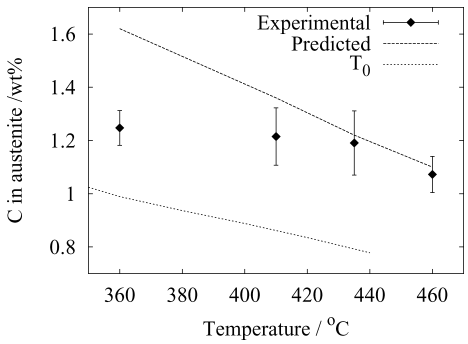

Fig. 4. Experimental and predicted austenite carbon content after transformation for steel B.

4. Conclusion

A model for the bainite reaction kinetics has been developed. This model takes into account the effects of the composition and austenite grain size, of the different nucleation sites, of the carbon partitioning and inhomogeneous redistribution, of the formation of carbon enriched austenite films between bainite sub-units and also of the varying dimensions of the forming bainite sub-units with temperature, austenite composition and yield strength. The model also takes into account the effect of the stress state resulting from transformation in the case of small austenite grains. As more work is still required, this effect is described using a semi-empirical equation function of the austenite yield strength. The same equation has been used for several alloys with the same small austenite grain size but different composition with equally good results. On the other hand, the decreasing mobility of carbon with decreasing temperature needs to be addressed in future models. The model has been applied to published data and its predictions show remarkable agreement over a large interval of temperature and grain size.

Acknowledgements

D. Gaude-Fugarolas acknowledges the Fonds Spéciaux de Recherches of the UCL, and P. J. Jacques acknowledges the Fonds National de la Recherche Scientifique (Belgium)

for the support of this work.

REFERENCES

1) H. I. Aaronson: Institute of Metals Monograph and Report Series No. 33, Institute of Metals, London, (1969), 270.
2) H. H. D. H. Bhadeshia: *Acta Metall.*, **29** (1981), 1117.
3) G. R. Purdy and M. Hillert: *Acta Metall.*, **32** (1984), 823.
4) S. van der Swaag and J. Wang: *Scr. Mater.*, **47** (2002), 169.
5) G. I. Rees and H. K. D. H. Bhadeshia: *Mater. Sci. Technol.*, **8** (1992), 985.
6) G. I. Rees and H. K. D. H. Bhadeshia: *Mater. Sci. Technol.*, **8** (1992), 994.
7) D. Quidort and Y. J. M. Brechet: *ISIJ Int.*, **42** (2002), 1010.
8) H. Matsuda and H. K. D. H. Bhadeshia: *Proc. R. Soc.* (*London*), **A460** (2004), 1710.
9) H. K. D. H. Bhadeshia: Bainite in steels, The Institute of Materials, London, (2001), 129.
10) A. Kutsov, Y. Taran, K. Uzlov, A. Krimmel and M. Evsyukov: *Mater. Sci. Eng. A*, **A273**–**275** (1999), 480.
11) P. J. Jacques, E. Girault, J. van Humbeeck, E. Aernoudt and F. Delannay: *J. Phys. IV France*, **7** (1997), C5-459.
12) Yu. N. Taran, K. I. Uzlov and A. Yu. Kutsov: *J. Phys. IV France*, **7** (1997), C5-429.
13) T. C. Tszeng: *Mater. Sci. Eng. A*, **A293** (2000), 185.
14) N. A. Chester and H. K. D. H. Bhadeshia: *J. Phys. IV France*, **7** (1997), C5-41.
15) V. M. Khlestov, E. V. Konopleva and H. J. McQueen: *Can. Metall. Q.*, **35** (1996), 169.
16) A. Ali and H. K. D. H. Bhadeshia: *J. Mater. Sci.*, **28** (1993), 3137.
17) S. B. Singh and H. K. D. H. Bhadeshia: *Mater. Sci. Eng. A*, **A245** (1998), 72.
18) J. Wang, S. van der Swaag, Z. Yang and H-S. Fang: *Mater. Lett.*, **45** (2000), 228.
19) J. W. Christian: Theory of Transformations in Metals and Alloys, Part I, Pergamon Press, Oxford, (1975), 1.
20) P. J. Jacques: *J. Phys. IV France*, **112** (2003), 297.
21) A. Matsuzaki and H. K. D. H. Bhadeshia: *Mater. Sci. Technol.*, **15** (1999), 518.
22) A. Lambert-Perlade, A. F. Gourgues and A. Pineau: *Acta Mater.*, **52** (2004), 2337.
23) R. H. Goodenow, R. H. Barkalow and R. F. Hehemann: *ISI Spec. Rep. 93*, (1969), 135.
24) S. V. Radclive and E. C. Rollason: *JISI*, **191** (1959), 56.
25) C. E. Ericsson, M. S. Bhat, E. R. Parker and V. F. Zackay: *Metall. Trans.*, **7A** (1976), 1800.
26) R. T. Howard and M. Cohen: *Trans. AIMME*, **176** (1948), 384.
27) S. B. Singh and H. K. D. H. Bhadeshia: *Mater. Sci. Technol.*, **12** (1996), 610.
28) S. B. Singh: PhD Thesis, University of Cambridge. Department of Materials Science and Metallurgy, Cambridge, (1998).
29) D. Gaude-Fugarolas and P. Jacques: Solid-Solid Phase Transformations in Inorganic Materials 2005–Phoenix (U.S.A.), (2005).
30) P. Jacques, E. Girault, T. Catlin, N. Geerlofs, T. Kop, S. van der Zwaag and F. Delannay: *Mater. Sci. Eng. A*, **A273**–**275** (1999), 475.
31) E. Girault, P. Jacques, P. Ratchev, J. Van Humbeeck, B. Verlinden and E. Aernouldt: *Mater. Sci. Eng. A*, **A273**–**275** (1999), 471.
32) Materials Science and Metallurgy Department–University of Cambridge and National Physical Laboratory. Materials Algorithms Project. University of Cambridge, http://www.msm.cam.ac.uk/map/mapmain.html, 1995. (Last Accessed 2005)